Subtropics-Related Interannual Sea Surface Temperature Variability in the Central Equatorial Pacific

JIN-YI YU AND HSUN-YING KAO*

Department of Earth System Science, University of California, Irvine, Irvine, California

TONG LEE

Jet Propulsion Laboratory, California Institute of Technology, Pasadena, California

(Manuscript received 1 April 2009, in final form 6 January 2010)

ABSTRACT

Interannual sea surface temperature (SST) variability in the central equatorial Pacific consists of a component related to eastern Pacific SST variations (called Type-1 SST variability) and a component not related to them (called Type-2 SST variability). Lead–lagged regression and ocean surface-layer temperature balance analyses were performed to contrast their control mechanisms. Type-1 variability is part of the canonical, which is characterized by SST anomalies extending from the South American coast to the central Pacific, is coupled with the Southern Oscillation, and is associated with basinwide subsurface ocean variations. This type of variability is dominated by a major 4–5-yr periodicity and a minor biennial (2–2.5 yr) periodicity. In contrast, Type-2 variability is dominated by a biennial periodicity, is associated with local air–sea interactions, and lacks a basinwide anomaly structure. In addition, Type-2 SST variability exhibits a strong connection to the subtropics of both hemispheres, particularly the Northern Hemisphere. Type-2 SST anomalies appear first in the northeastern subtropical Pacific and later spread toward the central equatorial Pacific, being generated in both regions by anomalous surface heat flux forcing associated with wind anomalies. The SST anomalies undergo rapid intensification in the central equatorial Pacific through ocean advection processes, and eventually decay as a result of surface heat flux damping and zonal advection. The southward spreading of trade wind anomalies within the northeastern subtropics-to-central tropics pathway of Type-2 variability is associated with intensity variations of the subtropical high. Type-2 variability is found to become stronger after 1990, associated with a concurrent increase in the subtropical variability. It is concluded that Type-2 interannual variability represents a subtropical-excited phenomenon that is different from the conventional ENSO Type-1 variability.

1. Introduction

The El Niño–Southern Oscillation (ENSO) is one of the strongest variations in the climate system and dominates interannual variability in the tropical Pacific. It is characterized by sea surface temperatures (SST) anomalies extending from the eastern to central equatorial Pacific. Prevailing ENSO theories, such as the delayed-oscillator theory (Schopf and Suarez 1988; Suarez and Schopf 1988; Battisti and Hirst 1989), suggest that surface wind anomalies in the western-to-central Pacific induce eastward propagating Kelvin waves that initiate ENSO events in the eastern equatorial Pacific. The Bjerknes feedback mechanism (Bjerknes 1966, 1969) then kicks in to amplify the SST anomalies and spread them westward to the central equatorial Pacific. As such, SST variations in the central equatorial Pacific are often considered an extension of SST anomalies in the eastern Pacific and thus part of the ENSO SST structure. However, recent studies have begun to emphasize central Pacific anomalies in separating different tropical Pacific warming/cooling events. Trenberth and Stepaniak (2001) were among the first to suggest that the SST contrast between the eastern and central Pacific be used to characterize different ''flavors'' of El Niño events. They proposed using a Trans-Niño Index (TNI) to portray the SST gradient along the equatorial Pacific. By analyzing the lead–lagged correlation between

* Current affiliation: Earth and Space Research, Seattle, Washington.

Corresponding author address: Dr. Jin-Yi Yu, Dept. of Earth System Science, University of California, Irvine, CA 92697-3100.
E-mail: jyyu@uci.edu

DOI: 10.1175/2010JCLI3171.1

the TNI and Niño-3.4 (5°S–5°N, 170°–120°W) SST index, they were able to better describe the ENSO propagation during the past hundred years. Larkin and Harrison (2005) also noticed several Pacific warming events had SST anomalies concentrated near the date line without major warming in the cold tongue region of the eastern Pacific. They named these events ''Dateline El Niño'' and showed that precipitation and temperature anomaly composites for these events were different than those of conventional El Niño.

The study of Yu and Kao (2007) first raised the possibility that the interannual SST variability in the central and eastern Pacific may involve different physical processes. By analyzing the persistence barrier in interannual SST anomalies, they noted that the decadal changes in the timing of the barrier are different in these two regions of the equatorial Pacific. In the eastern Pacific, the persistence barriers of the Niño-1 + 2 (10°S–0°, 80°–90°W) and Niño-3 (5°S–5°N, 90°–150°W) SST indices occurred during spring before 1976–77, shifted to summer between 1978 and 1988, and moved back to spring after 1988. No such decadal changes were found for the persistence barriers of both the Niño-3.4 and Niño-4 (5°S–5°N, 160°E–150°W) SST indices. These different decadal variations lead Yu and Kao (2007) to postulate that SST variations in the eastern and central equatorial Pacific are controlled by separate physical processes. To further examine the distinct behaviors of SST variability in these two parts of the Pacific, Kao and Yu (2009) used a method combining linear regression and empirical orthogonal function (EOF) analysis to separate the SST variability centered in the central equatorial Pacific from that in the eastern equatorial Pacific. They found different spatial patterns, evolutions, periodicities, and teleconnections between these two types of SST variability. Similarly, Ashok et al. (2007) and Kug et al. (2009) have also argued that some warming events in the central Pacific behave differently from conventional El Niño events (Rasmusson and Carpenter 1982) centered in the eastern Pacific.

These recent studies suggest the need to further look into the interannual SST variability in the central equatorial Pacific. This study aims to separate the central Pacific SST variability into a component linked to, and a component independent of, the conventional ENSO SST variability in the eastern Pacific and to identify the underlying generation mechanisms. For this purpose, lead–lagged regression and near-surface-layer heat budget analyses are performed. This paper is organized as follows: The reanalysis and ocean assimilation products used in this study are described in section 2. The ENSO-related and non-ENSO-related types of central Pacific SST variability are defined and their spatial and temporal properties contrasted in section 3. An analysis of the ocean surface-layer heat budget is presented in section 4 to identify processes that control these two types of SST variability. The tropical–subtropical interactions associated with the non-ENSO-related variability are examined further in section 5. The results are summarized and discussed in section 6.

2. Datasets

The major dataset used in this study is the ocean data assimilation product from the German Estimating the Circulation and Climate of the Ocean project (GECCO) (Kohl et al. 2006). It is used for analyses of the subsurface ocean structures and for near-surface ocean temperature budget analyses. The product is available for the period from 1952 to 2001. GECCO is produced by constraining the Massachusetts Institute of Technology (MIT) Ocean General Circulations Model (OGCM) with various observations using the adjoint method. This method corrects the initial state and the prior (first guess) surface forcing derived from the National Centers for Environmental Prediction (NCEP)–National Center for Atmospheric Research (NCAR) reanalysis (Kalnay et al. 1996) to improve the fit of the OGCM fields to various observations. The GECCO assimilation satisfies property conservation principles, which avoids the addition of artificial internal sources and sinks of properties (such as heat) in obtaining the estimated state. This assimilation process makes GECCO the most suitable assimilation product for ocean temperature budget analyses. The GECCO model covers a domain from 79.5°S to 79.5°N and has a $1° \times 1°$ horizontal resolution. It has 23 vertical levels with a thickness between adjacent levels that ranges from 5 to 5450 m. In this study, interannual anomalies are obtained by removing the mean seasonal cycle from the original fields and then applying a low-pass filter to suppress variations with time scales shorter than 12 months. The NCEP–NCAR reanalysis is used for the analyses of atmospheric fields.

3. Type-1 and Type-2 SST variability in the central Pacific

We use a linear regression-based method to separate Pacific interannual SST variability into a conventional-ENSO component and an ENSO-independent component. We first linearly regress all tropical Pacific SST anomalies with the SST anomalies averaged in an eastern Pacific box (5°S–5°N, 120°–80°W; see Fig. 1) where the maximum SST standard deviation is observed (not shown). The regressed SST anomalies are considered the conventional ENSO component of the variability. The residual SST anomalies obtained by removing the regressed anomalies from the original SST anomalies are

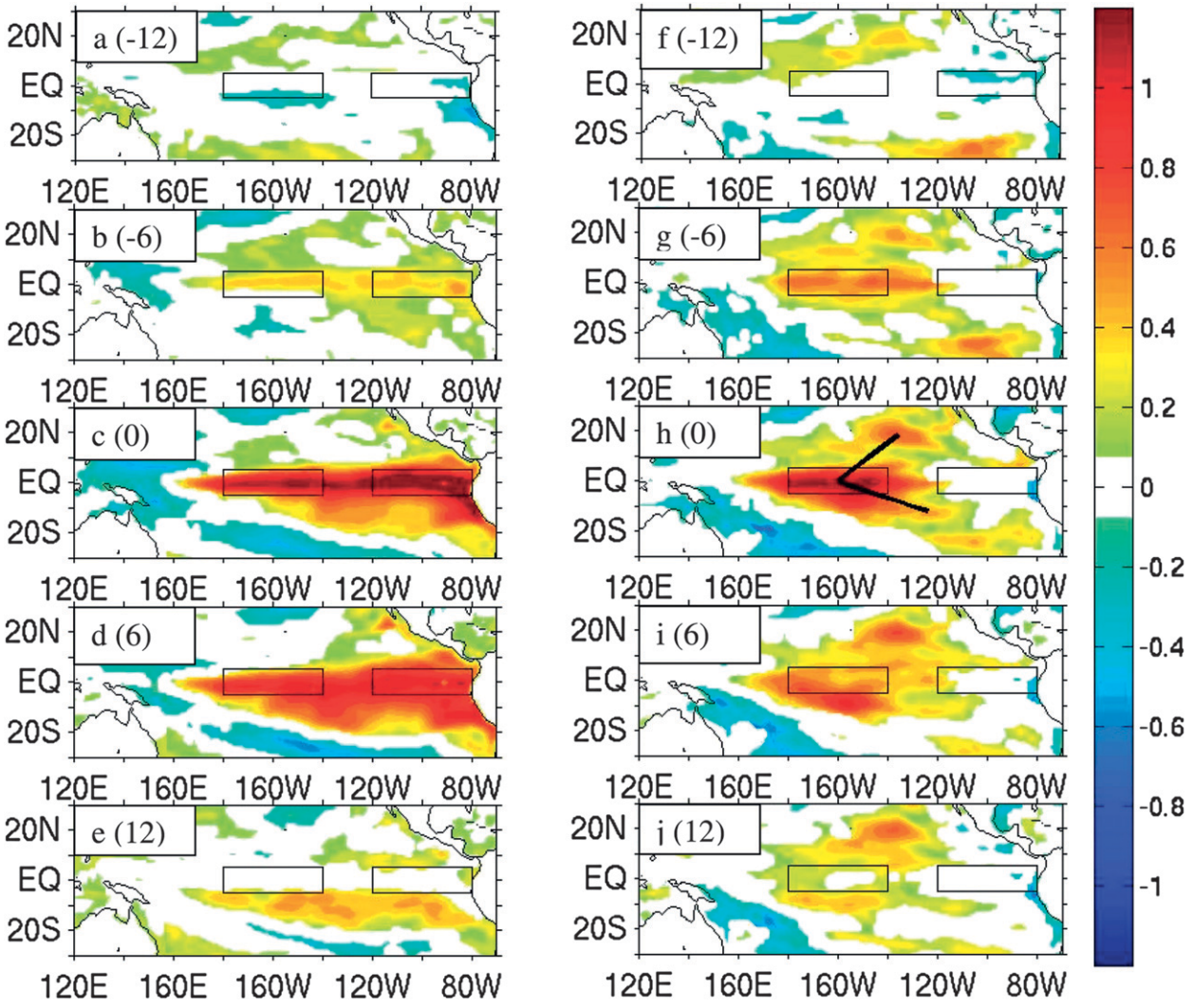

FIG. 1. Lead–lagged regression coefficients between SST anomalies in the tropical Pacific and the (a)–(e) Type-1 and (f)–(j) Type-2 SST indices. Contour intervals are 0.2°C month^{-1} °C^{-1}. The values in the parenthesis at the upper left indicate the lag months and the boxes denote the areas in the central and eastern Pacific used to define Type-1 and Type-2 indices. The black lines in (h) connect local maximum variability centers at 12°S and 18°N. Only coefficients exceeding the 95% confidence interval are shown.

considered the ENSO-independent component of the SST variability. We then average the ENSO-independent SST anomalies in a central Pacific box (5°S–5°N, 180°–140°W; see Fig. 1), where large standard deviations are found (not shown), to represent the strength of the ENSO-independent SST variability in the central Pacific. It should be noted that the central Pacific box is located near the SST anomaly center of the central Pacific type of ENSO identified and termed by Kao and Yu (2009, see their Fig. 3b). Similarly, the strength of the conventional ENSO SST variability in the central Pacific is represented by averaging the regressed SST anomalies in the same central Pacific box.

For the sake of convenience, we refer to the conventional ENSO part of the SST variability as Type-1 variability and the ENSO-independent part as Type-2 variability. We find that the standard deviation of Type-1 SST index is 0.69°C, while that of Type-2 SST index is 0.59°C. Type-1 is the more dominant type of interannual SST variability in the central Pacific, but Type-2 accounts for a comparable percentage of the variability. It should be noted that this way of separating Type-1 and Type-2 SST variability assumes linear dynamics dominates these two types of variability, an assumption whose validity is yet to be demonstrated. Nevertheless, the results presented in this study can be considered as a first-order examination of the ENSO and ENSO-independent SST variability in the central Pacific. Similar approaches were used in other studies of interannual-to-decadal SST variability in the Pacific, such as the studies of the

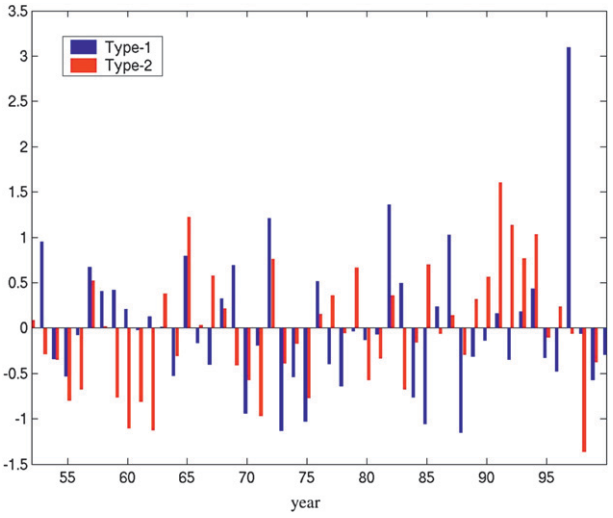

FIG. 2. Yearly variability of the Type-1 (blue) and Type-2 (red) SST indices from 1952 to 2001. The ordinate is the indices in °C.

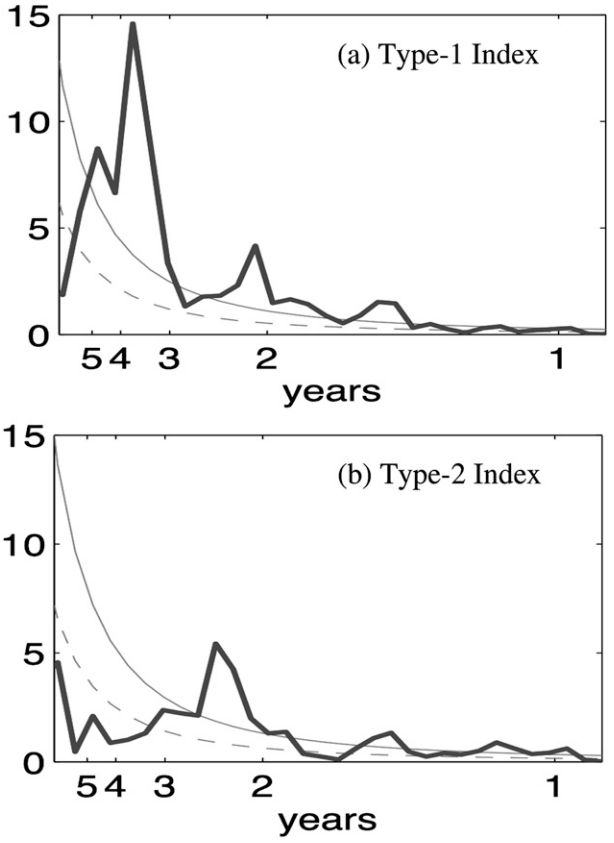

FIG. 3. Power spectra of the (a) Type-1 and (b) Type-2 SST indices. The solid (dashed) curves denote the 99% (95%) significance levels.

meridional mode by Vimont et al. (2003) and Chiang and Vimont (2004) and the Pacific decadal variability by Zhang et al. (1997). In our previous study, Kao and Yu (2009), a similar method was used to identify SST patterns associated with the central Pacific and eastern Pacific types of ENSO. Those patterns were found to be similar to those obtained using a nonlinear cluster analysis, which adds support to the appropriateness of using linear regression to separate Type-1 and Type-2 variability.

We next perform regression analyses between Type-1/Type-2 indices and SST anomalies in the tropical Pacific to construct the patterns and evolution of these two types of variability. The results are shown in Fig. 1. Only coefficients exceeding the 95% confidence interval based on a two-tailed Student's t test are shown. Type-1 variability (Figs. 1a–e) shows a conventional ENSO evolution (Rasmusson and Carpenter 1982) with SST anomalies emerging first in the cold tongue region, extending westward toward the date line, and decaying in the central Pacific. In contrast to Type-1, which has anomalies of the same sign in the central and eastern Pacific, Type-2 variability (Fig. 1h) has a positive anomaly pattern centered in the central Pacific but with weak negative anomalies in the eastern and western Pacific. Also in contrast to the Type-1 SST pattern, which is confined mostly to the equatorial region, the Type-2 pattern spreads over a wider latitudinal range and shows a strong association with the subtropics (Figs. 1f–j). Type-2 SST anomalies appear in the subtropics before the onset of SST anomalies along the equator. All of these differences indicate that the subtropical Pacific plays a more important role in Type-2 variability than in Type-1 variability. We have repeated the same regression analysis with the Met Office Hadley Centre's Sea Ice and Sea Surface Temperature dataset (HadISST) (Rayner et al. 2003) and obtained similar results (not shown).

Seasonal variations in the standard deviations of these two types of SST variability are examined to determine their phase locking to the seasonal cycle (not shown). Both types are weakest during the boreal spring. However, Type-1 has its maximum standard deviation during September–November while Type-2 has its maximum a bit later, during October–December. We average Type-1 and Type-2 indices respectively in September–November and October–December to represent their yearly strength. Figure 2 shows the relative strengths of these two types of variability from 1952 to 2001. It indicates that Type-2 events can occur alone (e.g., 1979, 1991, and 1998) or together with Type-1 events (e.g., 1965, 1972, and 1975). There are also years when only Type-1 events occur (e.g., 1987 and 1997). The leading periodicities of these two types of SST variability are examined in Fig. 3 using power spectral analysis. The Type-1 index has significant power in both the 4-yr and 2-yr bands, which are the known leading frequencies of ENSO (Rasmusson and

Carpenter 1982; Rasmusson et al. 1990; Barnett 1991; Gu and Philander 1995; Jiang et al. 1995; Wang and Wang 1996). The power spectrum of Type-2 index is dominated by a single peak near 2–2.5 years (Fig. 3b). We will explore this biennial periodicity further in section 5.

We next examine the atmosphere and ocean structures of these two types of variability in Fig. 4 by calculating the lead–lagged regression between the Type-1/Type-2 indices and SST, zonal wind stress, and sea surface height (SSH) anomalies along the equator. SST anomalies for Type-1 events appear first in the eastern Pacific and then extend westward toward the central Pacific (Fig. 4a), as indicated by the local maximum labeled by asterisks in the figure. In contrast, Type-2 SST anomalies are confined locally in the central Pacific and are associated with weakly out-of-phase SST anomalies in the cold tongue region (Fig. 4b). The anomalies appear to propagate eastward initially, then turn westward as the event develop to large amplitude. For Type-1, zonal wind stress anomalies in the western Pacific, which are essential to producing equatorial oceanic waves, show up before the onset of the events (around 12 months before the peak, Fig. 4c). No such strong wind anomalies are found in the western Pacific for Type-2 events (Fig. 4d). As shown in Figs. 4e and 4f, Type-1 SSH anomalies show an apparent eastward propagation across the Pacific basin, while Type-2 SSH anomalies exhibit weak and near-local fluctuations. The lack of a basinwide SSH anomaly propagation associated with the Type-2 variability is consistent with the absence of significant zonal wind stress anomalies in the western Pacific. To summarize, Type-1 events are characterized by basinwide evolutions of SST, zonal wind, and subsurface temperature structures (as reflected in the SSH fluctuations), which are well-known features of the conventional ENSO. Type-2 events, on the other hand, are characterized by local SST, zonal wind, and subsurface temperature variations in the central equatorial Pacific.

4. Near-surface-layer ocean temperature balance analysis

We next perform near-surface-layer ocean temperature budget analyses to identify the physical processes that control the Type-1 and Type-2 SST evolutions. The near-surface-layer temperature budget (McPhaden 2002; An and Jin 2004; Ye and Hsieh 2008) can be described by the following equation:

$$\frac{\partial T}{\partial t} = -\left(\overline{u}\frac{\partial T'}{\partial x} + u'\frac{\partial \overline{T}}{\partial x} + u'\frac{\partial T'}{\partial x}\right) - \left(\overline{v}\frac{\partial T'}{\partial y} + v'\frac{\partial \overline{T}}{\partial y} + v'\frac{\partial T'}{\partial y}\right) - \left(\overline{w}\frac{\partial T'}{\partial z} + w'\frac{\partial \overline{T}}{\partial z} + w'\frac{\partial T'}{\partial z}\right) + \frac{Q}{\rho_o C_p H} + R.$$

Here, T, u, v, w are respectively the temperature, zonal, meridional, and vertical current velocities in a near-surface layer of constant depth H. The overbars denote the climatological seasonal cycle, and the prime denotes the nonseasonal anomaly from the mean seasonal cycle. The first three groups of terms on the right-hand side of the equation represent the advection in zonal, meridional, and vertical directions, respectively. The term after the advection terms is the surface heat flux (SHF) term; Q is the total heat flux; ρ_o is seawater density; and C_p is the ocean heat capacity. Following Ye and Hsieh (2008), an average over a fixed depth is used for the temperature budget calculation in a near-surface layer. The depth is set to 50 m in the central equatorial Pacific and 20 m in the eastern equatorial Pacific, close to the climatological mixed layer depths in these regions. The last term, R, denotes the residual term, which includes vertical and horizontal diffusion as well as nonlinear terms due to the correlation of velocity and temperature gradient on submonthly time scales, for example, associated with tropical instability waves. The latter nonlinear term is included in the residual term because only monthly averaged fields are available from the GECCO product, so submonthly variability cannot be evaluated explicitly. Therefore, it is important to point out that the nonseasonal anomalies in the above equation only represent anomalies with time scales longer than a month. For illustration purposes, the interpretation of the temperature budget analyses is described for the warm phase only. Converse interpretations can be applied for the cold phase of the events.

To determine the relative importance of the tendency terms in the temperature budget, we calculate the lead–lagged regression of Type-1/Type-2 SST indices with each tendency term averaged over the equatorial eastern and central Pacific boxes, which are indicated in Fig. 1. Figure 5 shows the evolution of the tendency terms over these two boxes for Type-1 events. In both panels, lag 0 corresponds to the peak time of Type-1 SST variability in the central equatorial Pacific. For this type, large budget terms appear first in the eastern Pacific box (Fig. 5b) where the initial warming tendency is contributed by the vertical advection term (green curve). This reflects the importance of thermocline fluctuations and upwelling/downwelling activity to the eastern Pacific SST anomalies. These are related to remote Ekman pumping in the western central Pacific that

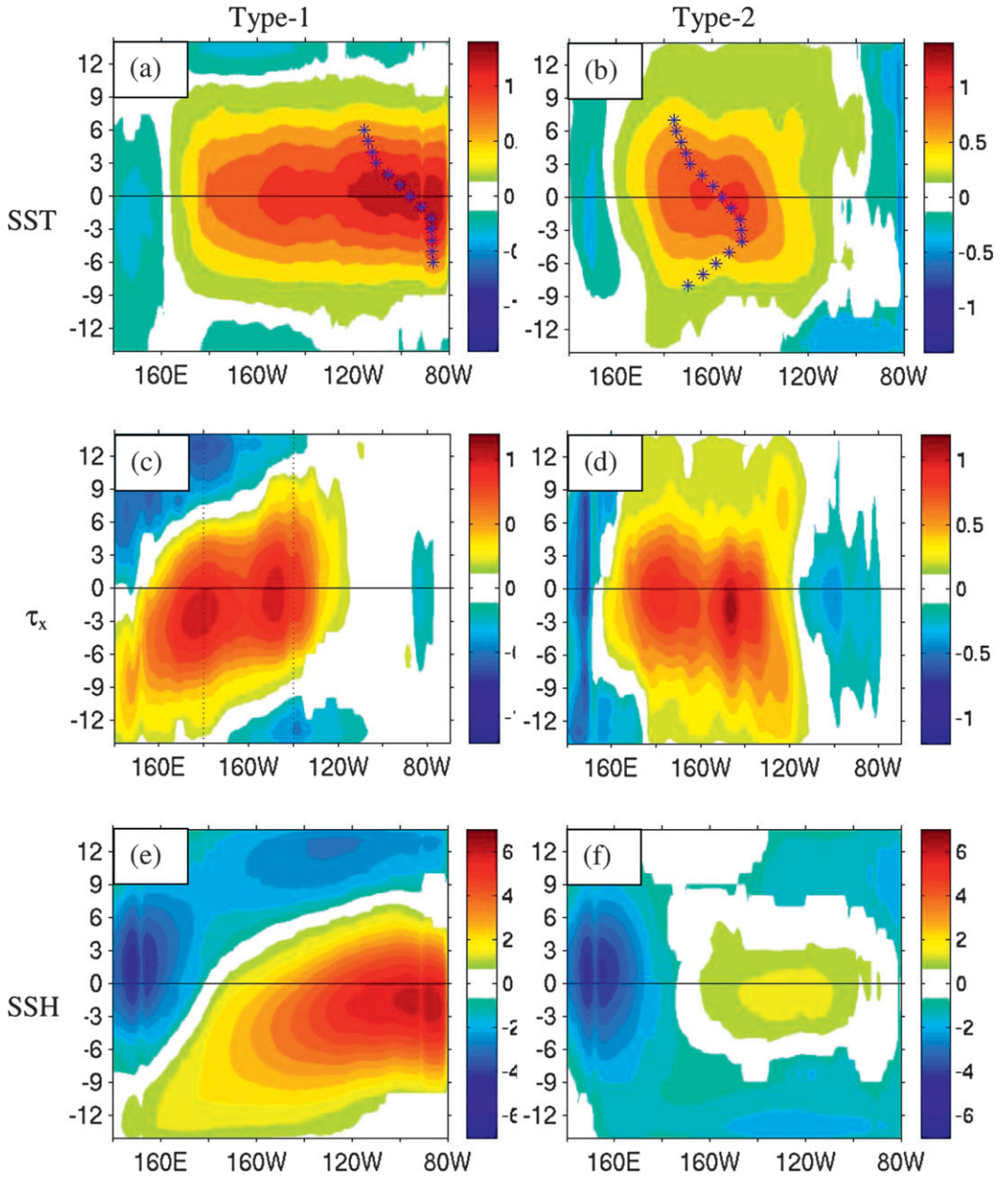

FIG. 4. Lead–lagged regression of (a),(b) SST, (c),(d) zonal wind stress, and (e),(f) SSH anomalies at the equator with the (left) Type-1 and (right) Type-2 SST indices. The contour intervals are 0.2°C month^{-1} °C^{-1}, 0.2 m s^{-1} month^{-1} °C^{-1}, and 1 cm month^{-1} °C^{-1}. The abscissa is the longitude and the ordinate shows the time lags in months. The asterisks in (a),(b) indicate the local maximum. Only coefficients exceeding the 95% confidence interval are shown.

cause equatorial Kelvin waves to propagate into the region as well as local Ekman pumping due to the variations in local trade winds. The early development of the vertical advection is consistent with the role of the Kelvin waves that often precede the mature phase of warm events in the eastern equatorial Pacific. The vertical advection term continues to play an important role throughout the SST evolution in the eastern Pacific region.

After the onset of SST anomalies, both the meridional advection term (red curve) and the SHF term (black curve) increase magnitude and become major terms in the temperature budget. These two terms tend to cancel each other because the former contributes a warming tendency, but the latter contributes a cooling tendency. The zonal advection term (blue curve) also contributes to the SST increases but its magnitude is smaller than the

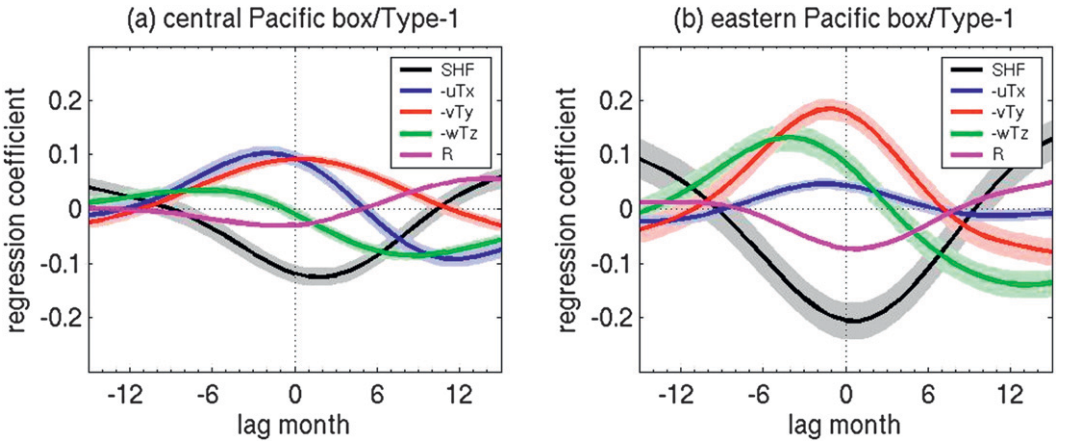

FIG. 5. Lead–lagged regression of the Type-1 index with surface-layer temperature tendency terms in the (a) central Pacific and (b) eastern Pacific. The black, blue, red, green, and magenta lines denote the air–sea SHF, zonal, meridional, vertical advection, and residual terms, respectively. The light shaded area shows the 95% confidence interval for each term.

meridional and vertical advection. It is noted that the amplitudes of SHF and zonal and meridional advection terms all increase and decrease together with the SST anomalies, reflecting local air–sea interaction processes. Only the vertical advection term shows an apparent phase lag from the SST evolution in the eastern Pacific. This phase relation is consistent with the delayed-oscillator theory, which suggests that thermocline variations control the onset and termination of ENSO SST anomalies. Overall, the results of the temperature budget analyses presented here are consistent with those reported by Yu and Mechoso (2001) using a coupled atmosphere–ocean GCM simulation and by Kim et al. (2007) using another assimilation product [Estimating the Circulation and Climate of the Ocean (ECCO)].

In the central Pacific box (Fig. 5a) zonal advection (blue) is the leading temperature tendency term for the Type-1 SST evolution. This term lags the vertical advection in the eastern Pacific box by about 3 months, suggesting the Type-1 central Pacific warming tends to follow the eastern Pacific temperature variations. The meridional advection (red) and SHF (black) terms again cancel each other and together have a small contribution to the development of the SST anomalies. Both the vertical advection (green) and residual (pink) terms are weak. Figures 5a and 5b together indicate that Type-1 events onset with a weakening/strengthening of the vertical advection over the cold tongue region and then expand into the central Pacific via zonal advection. In other words, the Type-1 SST variability in the central equatorial Pacific is produced by zonal advection of the thermocline-controlled SST anomalies from the eastern Pacific.

Figure 6 shows the evolution of the regressed temperature tendency terms for Type-2 variability in the eastern and central Pacific boxes. In both panels, lag 0 corresponds to the time when the Type-2 SST variability peaks in the central equatorial Pacific. In contrast to Type-1, there are no large tendency terms in the eastern Pacific box (Fig. 6b), except for the SHF term (black curve). We find that most of the SHF term is contributed by shortwave radiation and latent heat fluxes. It is likely that the heating effect of the shortwave radiation is overestimated here; because our temperature tendency calculation does not consider solar penetration, it deposits all of the solar flux into the chosen surface layer. Large tendency terms develop primarily in the central Pacific box (Fig. 6a), suggesting that the Type-2 SST variability is not an extension of SST variability from the eastern equatorial Pacific.

Figure 6a shows that the initial warming in the central equatorial Pacific during Type-2 events is contributed mostly by the SHF term (black) and the vertical advection term (green). During the developing stage, the zonal (blue) and meridional (red) advection terms strengthen and become the leading contributors to the growth of temperature anomalies. It is important to note that both the meridional and vertical advection terms never change phase during the evolution, while the zonal advection term reverses its sign a couple of months after the peak of the events. These different phase relations suggest that the meridional and vertical advection terms are not involved in the decay of Type-2 events, but the zonal advection term is. The latter process is associated with anomalous westward advection of cold tongue water toward the central equatorial Pacific during the termination of a warm event and the initiation of a cold event. In fact, we find that all the linear advection terms for Type-2 are dominated by the advection of mean temperature

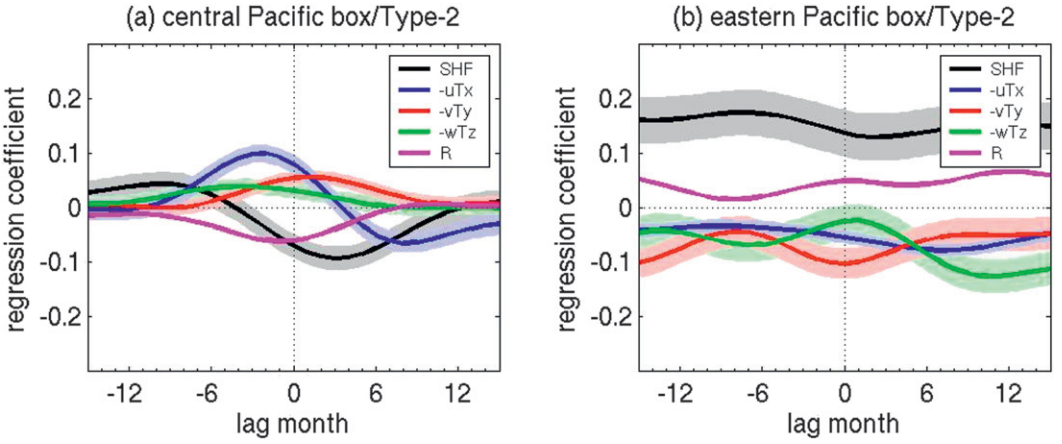

FIG. 6. As Fig. 5 but for regression with Type-2 SST index.

gradients by anomalous currents (not shown). This finding suggests that surface wind variations, which induce the surface current anomalies, are important in the evolution of Type-2 SST variability. Figure 6a shows that SHF is another important term contributing to the decay of Type-2 events. The residual term (pink) has a cooling effect throughout the evolution and is consistent with the effects of vertical diffusion.

As noted in Fig. 1, Type-2 SST anomalies show up first in the northeastern subtropical Pacific and then extend southwestward to the central equatorial Pacific. To understand how the anomalies spread equatorward, we examine the regressed temperature tendency terms along a north–south meridional path that links the local Type-2 SST anomaly centers at 18°N and 12°S. The black lines in Fig. 1h show this path. Figure 7 shows the meridional evolution of the near-surface-layer temperature tendency and the tendency terms along this path. The abscissa shows the lagged months from 18 months before to 18 months after the peak of a Type-2 event. Based on the temperature tendency term (Fig. 7a), we can separate the Type-2 evolution into three major periods. During lags of −18 to −9 months (the onset period), the warming appears first in the northern subtropics around 10°–15°N and then spreads toward the equator. During lags of −9 to 0 months (the growth period), the equatorial warming is enhanced rapidly and its latitudinal width expands. During lags of 0 to 9 months (the decay period), the temperature tendency term becomes negative.

We now focus on identifying the physical processes responsible for the temperature evolution in each of the three periods. During the onset period, the temperature budget analysis shows that the SHF term is responsible for the initial warming in the northern subtropics (Fig. 7b). The southward spreading of the warming is also due mostly to the SHF term. Near the equator, both the meridional and vertical advection terms (Figs. 7d,e) produce warming tendencies, but most of the warming is cancelled out by a cooling tendency from the zonal advection term (Fig. 7c). Rapid growth of the equatorial SST anomalies starts after the subtropical warming arrives at the equator around lag −9 and lasts until lag 0. During this growth period, all three ocean advection terms increase and contribute to the intensification of SST anomalies. The zonal advection term becomes the most important term and dominates the equatorial warming until the temperature anomaly reaches its peak intensity (Fig. 7c). The meridional advection term is also large and is particularly important in increasing the latitudinal extent of the warming. As mentioned earlier, Type-2 variability is dominated by anomalous current advection of climatological temperature gradients. The larger warming effect of meridional advection off the equator is consistent with the larger climatological meridional temperature gradients off than at the equator. The vertical advection term (Fig. 7d) also produces a warming tendency but is large only near the equator.

During the decay period, both the SHF (Fig. 7a) and zonal advection terms (Fig. 7c) contribute to the decay of temperature anomalies. The large latitudinal extent of the SHF term is consistent with the latitudinal width of the Type-2 SST anomalies during their peak phase (see Fig. 1h). This indicates that thermal damping is the main process that terminates Type-2 events. The residual term (Fig. 7f) has little contribution during all three periods, suggesting that the diffusion term and submonthly variations play a minor role in Type-2 events. Based on the analysis of Fig. 7, we can consider Type-2 SST variability a local coupled variability in the central equatorial Pacific triggered by subtropical forcing.

To further establish the validity of the regression results presented in Fig. 7, we perform a case study using the

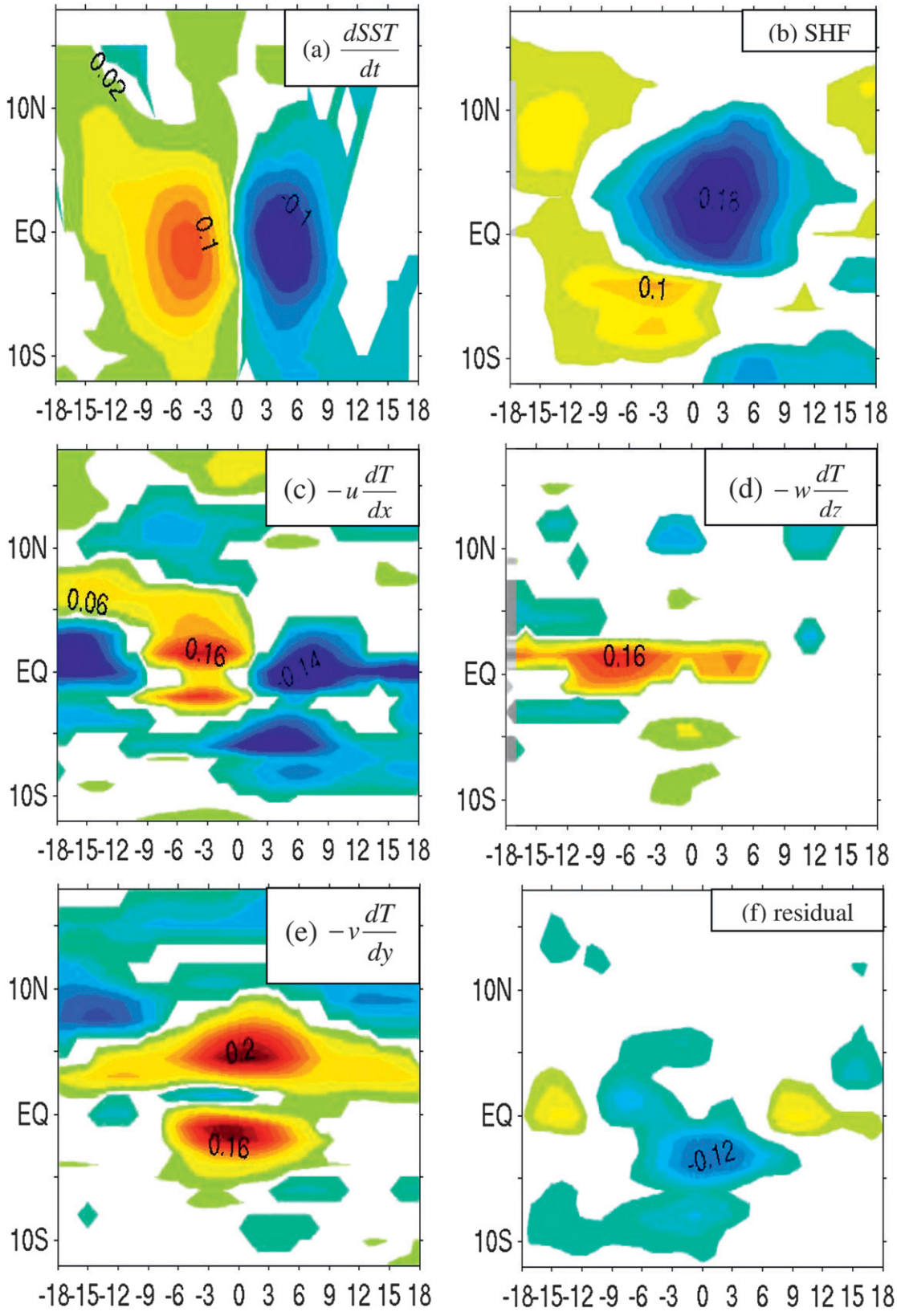

FIG. 7. Meridional evolution of the regressed surface-layer temperature tendency terms for Type-2 SST events along the black lines in Fig. 1h: (a) SST tendency, (b) SHF, (c) $-u\ dT/dx$, (d) $-w\ dT/dz$, (e) $-v\ dT/dy$, and (f) residual. Contour intervals are 0.02°C month^{-1} °C^{-1}. Only coefficients exceeding the 95% confidence interval are shown.

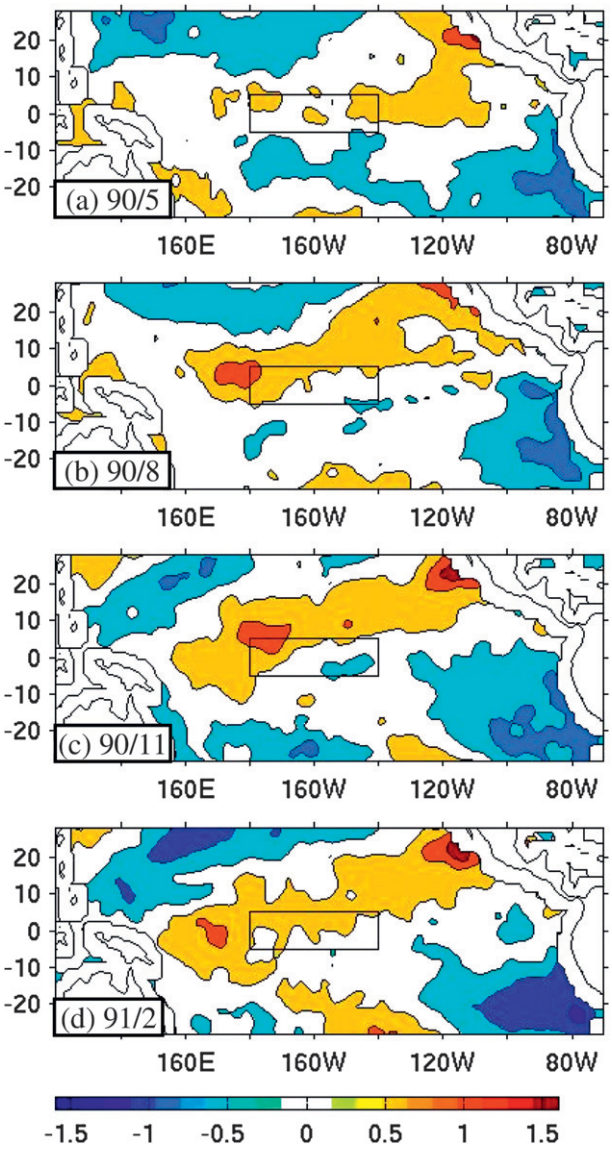

FIG. 8. Evolution of SST anomalies in the tropical Pacific from May 1990 to February 1991. The contour interval is 0.5°C. The "year/month" are indicated in the bottom left of the panels.

1990–91 warming event, which is a pure Type-2 event, as indicated in Fig. 2. Figure 8 shows the evolution of SST anomalies from May 1990 to February 1991. It shows that positive SST anomalies in this event appeared first in the northeastern subtropics in May 1990 (Fig. 8a), gradually extended to the central equatorial Pacific (Fig. 8b), and had formed an anomaly pattern linking the northeastern subtropics to the central tropics by August 1990 (Fig. 8c). As the event evolved into its peak phase in February 1991 (Fig. 8d), a rotated V-shaped SST anomaly pattern was established and extended from central equatorial Pacific into the subtropics of both hemispheres. The near-surface layer temperature budget analysis for this event along the same meridional path used for Fig. 7 is shown in Fig. 9. The figure indicates that the SHF term initiates the warming around 10° to 15°N at the beginning of the event (Fig. 9a), consistent with Fig. 7b. Similar to the regressed tendency analysis, the rapid development of equatorial SST anomalies (during August 1990–February 1991) are contributed by all three ocean advection terms (Figs. 9b–d) with the zonal advection being the strongest one. Slightly different from the regressed tendency analysis, the meridional advection term increases earlier and contributes to the early development of this particular event. But, in general, the pattern and evolution of the meridional advection term are consistent with those revealed by the regressed analysis. For example, the meridional term peaks off equator, similar to that shown in Fig. 7e. The temperature budget analysis of the 1990–91 Type-2 event is, in general, consistent with the regressed budget analysis.

5. Tropical and subtropical linkage for Type-2 variability

The temperature budget analysis indicates that surface heat flux forcing initiates SST anomalies in the subtropics and spreads them southward to trigger Type-2 SST variability at the equator. Ocean advection terms aid the onset and development of SST anomalies in the central equatorial Pacific. Both the surface heat flux forcing and the ocean advection anomalies can be related to anomalous atmospheric wind forcing. We find latent heat fluxes to be the leading contributor to the surface heat flux anomalies (not shown). Meridional advection (Fig. 7e) by Ekman currents and vertical advection (Fig. 7d) by local Ekman pumping that impact the central Pacific SST may both be associated with variations in the strength of shallow meridional overturning circulations, often referred to as the subtropical cell or STC (after McCreary and Lu 1994). The subsurface branch of the STC (the equatorward pycnocline flow) has an interior pathway that connects the central equatorial Pacific with the subtropical regions (e.g., Fig. 2 of Lee and Fukumori 2003). Variations in subtropical trade winds could cause an oscillation of the STC, which involves variations in the poleward Ekman current at the surface, the equatorward pycnocline flow, and the upwelling that connects the two. It is conceivable that the oscillation of the STC in response to trade wind variations would affect the meridional and vertical advective tendencies of the upper-ocean temperature in the central equatorial Pacific.

The importance of trade wind variations during the onset period of Type-2 SST variability is verified in Fig. 10, which shows the evolution of zonal wind stress, meridional

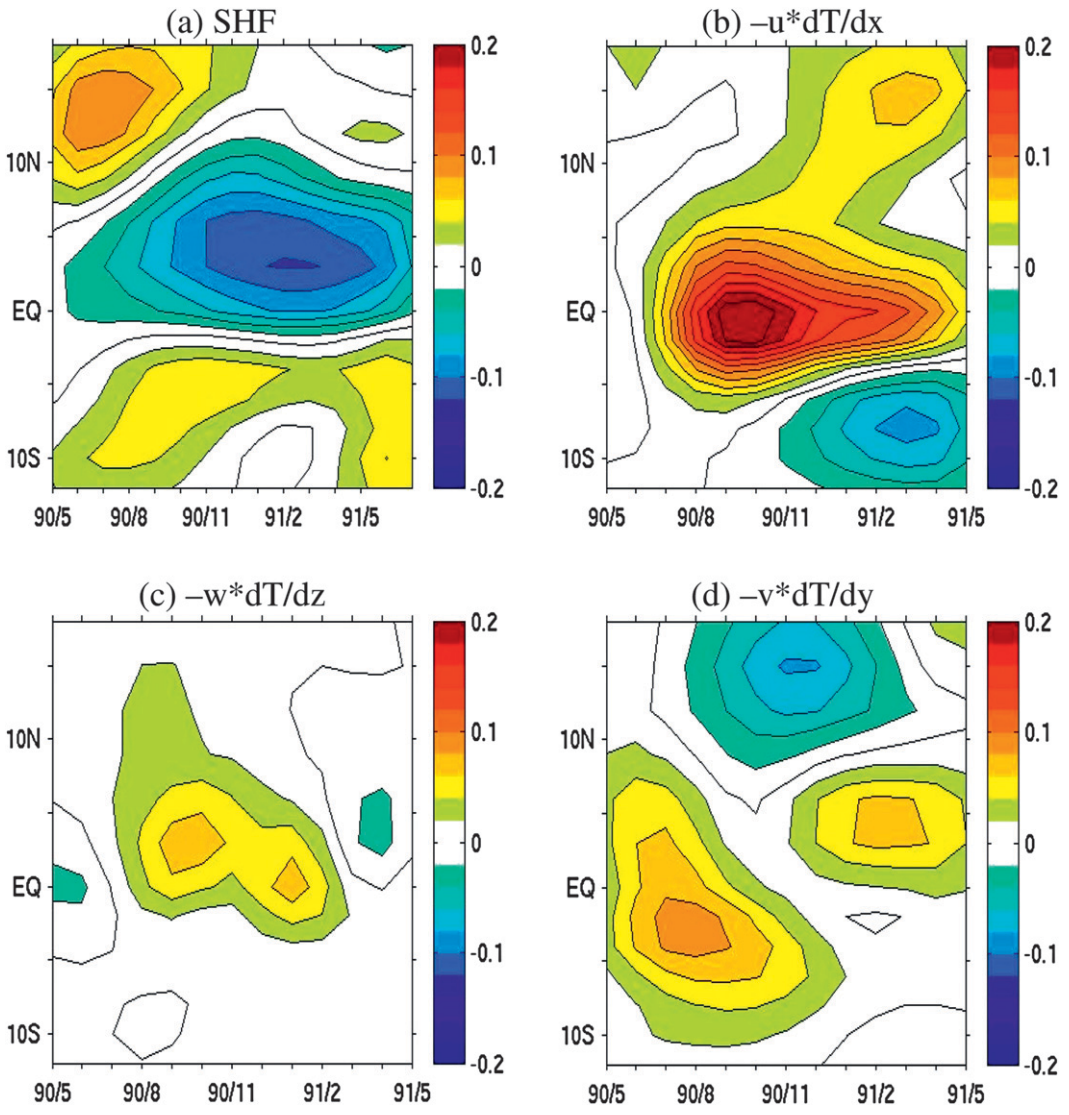

FIG. 9. Meridional evolution of the surface-layer temperature tendency terms along the black lines in Fig. 1h for the 1990 event: (a) SHF, (b) $-u\,dT/dx$, (c) $-w\,dT/dz$, and (d) $-v\,dT/dy$. The evolutions are shown for the period from May 1990 to May 1991. Contour intervals are 0.02°C month^{-1}.

wind stress, and sea level pressure (SLP) anomalies along the meridional path where we analyzed the ocean temperature budget. During the onset period, large surface westerly and southerly wind stress anomalies appear from 20° to 5°N (Figs. 10a,b), which weaken the climatological northeasterly trade winds, reduce surface evaporation, and produce a tendency toward positive SST anomalies. The wind stress anomalies are particularly intensified during lags −12 to −6 months, when the anomalies spread southward. The SLP anomalies (Fig. 10c) also intensify and extend southward during this period. One possible explanation for these coherent variations is that a forcing external to the Type-2 variability controls the subtropical SLP variations, which then cause the trade wind anomalies to intensify and spread equatorward. The possible external forcing for the SLP variations is discussed later. As the surface wind stress anomalies arrive at the equator, the weakened trade winds reduce the upwelling of cold subsurface ocean water and reduce the northward advection of warm SSTs through Ekman transport. As a result, a warming starts at the equator (recall Figs. 7d,e). At the same time, the positive zonal wind stress anomalies induce eastward current anomalies, which facilitate the intrusion of warmer western Pacific waters into the central equatorial Pacific. Figure 10 shows that, as the Type-2 SST anomalies develop in the central equatorial

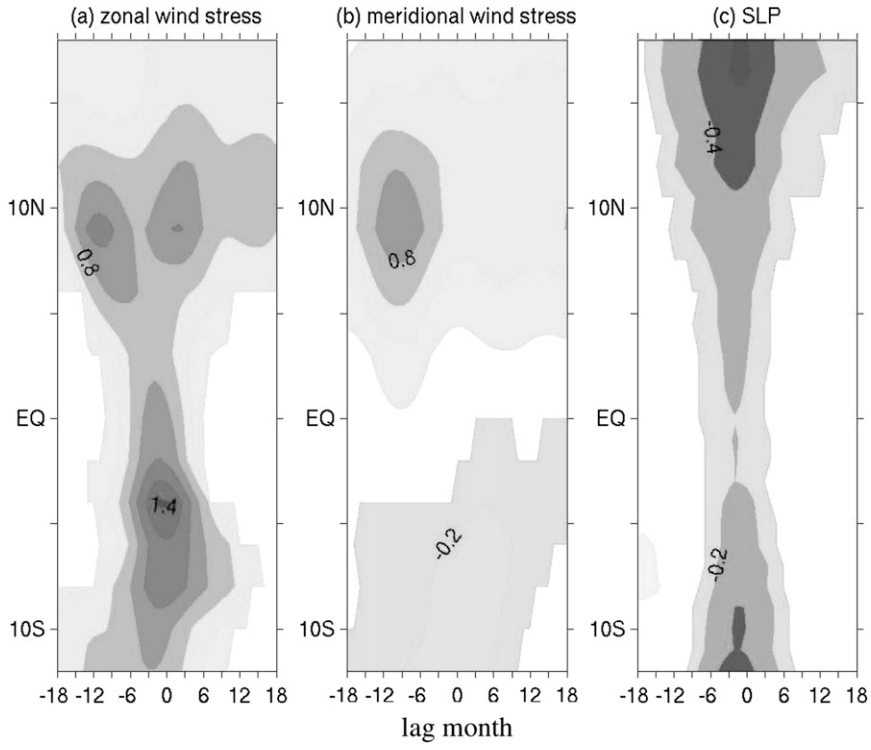

FIG. 10. Meridional evolutions of Type-2 (a) zonal wind stress, (b) meridional wind stress, and (c) SLP along the black lines in Fig. 1h. Contour intervals are 0.2 cm s^{-1} $month^{-1}$ $°C^{-1}$ for wind stress and 0.2 mb $month^{-1}$ $°C^{-1}$ for SLP.

Pacific, SLP anomalies in both hemispheres intensify and spread both zonal and meridional wind anomalies equatorward.

The above analyses indicate that SLP variations control surface wind anomalies and are particularly important to Type-2 SST variability. In Fig. 11, we contrast the SLP anomaly patterns associated with Type-1 and Type-2 SST variability. The values shown in the figure are the correlation coefficients between SLP anomalies (from the NCEP–NCAR reanalysis) and the Type-1 and Type-2 SST indices. Figure 11a shows that, as expected, Type-1 SST variability is associated with a Southern Oscillation pattern characterized by out-of-phase SLP anomalies between the eastern and western tropical Pacific. The SLP variations over the Maritime Continent region are linked to SLP over the eastern equatorial Pacific through the Walker circulation. Figure 11b shows that the SLP anomaly pattern associated with Type-2 variability does not resemble the Southern Oscillation. Instead, the SLP variations over the Maritime Continent are linked to SLP variations in the subtropics of both the North and South Pacific, suggesting that a connection through local Hadley circulation may be more important. We notice that the center of the subtropical SLP anomalies in the Northern Hemisphere is located at the southern boundary of the mean wintertime subtropical high (not shown). Therefore, the SLP anomalies shown in Fig. 11b represent variations in the extension and strength of the northern subtropical high. We find that the power spectrum of a subtropical high index, which is defined as the SLP anomalies averaged in the northeastern subtropics (20°–40°N, 160°–110°W), also shows a significant peak in a 2–2.5-yr band (Fig. 12). This peak is consistent with the dominant periodicity found for Type-2 SST index (see Fig. 3b), and further suggests there is a close linkage between the interannual SST variability in the northeastern subtropical Pacific and central equatorial Pacific.

The results presented so far indicate that subtropical forcing plays an important role in producing Type-2 SST variability in the tropics and that this type of variability is as important as Type-1 SST variability in producing interannual warming and cooling in the central Pacific. We also notice from Fig. 2 that Type-2 SST variability undergoes decadal/interdecadal variations. The variations can also be seen in Fig. 13, which shows the SST standard deviation along the northeastern subtropical-to-central equatorial Pacific pathway (i.e., the black lines shown in Fig. 1h) from 1952 to 2001 using a 10-yr running window. It shows that the SST variability in the northern subtropics is stronger in the 1960s and 1990s but weaker in

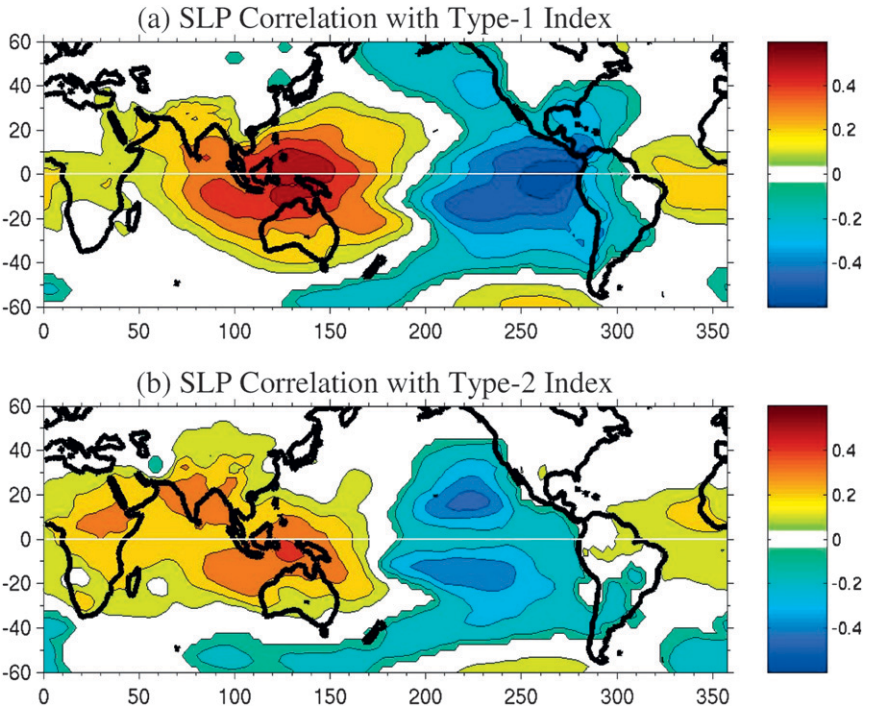

FIG. 11. Correlation coefficients of sea level pressure with (a) Type-1 and (b) Type-2 SST indices. The contour interval is 0.1. Only coefficients exceeding the 95% confidence interval are shown.

the 1970s and 1980s. This decadal change in subtropical SST variability is in accordance with the decadal variability in Type-2 events revealed in Fig. 2, which shows Type-2 events have been more intense and more frequent beginning during the 1990s. This result suggests that there is decadal/interdecadal variability in subtropical SST interannual variations and their forcing of the central equatorial Pacific and that Type-2 SST variability has become more active since 1990.

6. Conclusions and discussion

In this study, we focused on analyzing interannual SST variability in the central equatorial Pacific. We separated this variability into a Type-1 variability that is related to the eastern equatorial Pacific and a Type-2 variability that is not. Type-1 variability is part of the conventional ENSO that emerges in the eastern Pacific. In contrast, Type-2 variability is found to have a strong connection to the subtropical Pacific. Analyses of the surface-layer ocean temperature budget were performed to identify the leading physical processes for these two types of SST variability. The results show that, as expected, Type-1 variability in the central Pacific results from the zonal advection of thermocline-controlled SST variations from the eastern equatorial Pacific. The Type-2 variability is linked to the northeastern subtropics through surface wind forcing and associated atmosphere–ocean heat fluxes (primarily the latent heat flux) and surface ocean advection. This study suggests that there is a distinct interannual SST variability in the central equatorial Pacific that is

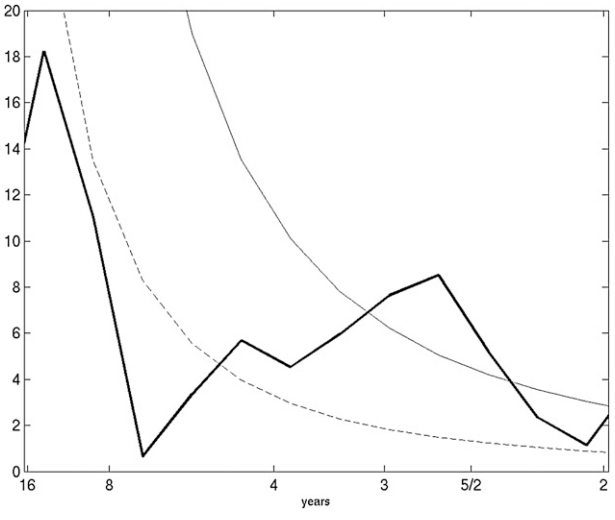

FIG. 12. Power spectrum of subtropical high variability calculated from the sea level pressure anomalies averaged in the area between 20°–40°N and 160°–110°W. The thin line denotes the 95% significance level and the dashed line denotes the red-noise spectrum.

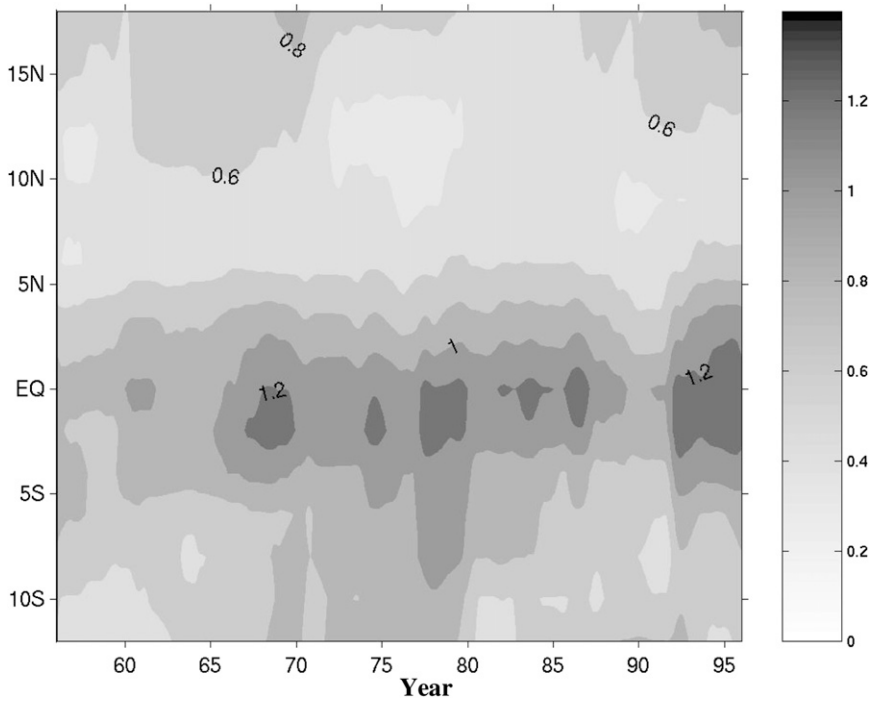

FIG. 13. The standard deviations of SST anomalies along the black lines in Fig. 1h from 1958 to 2001 calculated with a 10-yr running window. Contour interval is 0.2°C. The abscissa shows the years.

not related to basinwide equatorial thermocline variations, but to subtropical forcing, and that this Type-2 variability has been strengthened since 1990. Our study also reaffirms the suggestion from earlier studies, such as Vimont et al. (2003), Anderson (2003), Chang et al. (2007), that a significant part of the interannual SST variability in the equatorial Pacific is related to subtropical forcing.

The Type-2 SST variability discussed here is basically the same as the central Pacific (CP) type of El Niño first discussed by Kao and Yu (2009), both of which have their SST anomalies centers located in the equatorial central Pacific (cf. Fig. 1h to their Fig. 3b). The correlation coefficient between our monthly Type-2 index and their monthly CP index is 0.70. The Type-1 SST variability is part of their eastern Pacific (EP) type of El Niño, which they considered to be the conventional ENSO in that the SST anomalies extend from the South American coast toward the central Pacific. By analyzing the associated atmospheric and oceanic structures, Kao and Yu (2009) concluded that the CP type is a local atmosphere–ocean coupling phenomenon while the EP type is a basinwide coupling phenomenon. Our study confirms their suggestion that the CP type of tropical Pacific warming has a different generation mechanism from the EP type. Our analyses not only identify the relative importance of the various local coupling processes in the evolution of the CP El Niño but also demonstrate that those local processes are triggered by remote forcing from the subtropical Pacific. We should also point out that, in addition to the study of Kao and Yu (2009), Ashok et al. (2007) and Kug et al. (2009) also proposed generation mechanisms for this nonconventional type of El Niño. Ashok et al. emphasized wind-induced thermocline variations within the tropical Pacific for the SST evolution, while Kug et al. emphasized zonal advection in the ocean. Our results indicate that the ocean advection process is more important to the evolution of these nonconventional events, particularly during the growth period. However, vertical advection and surface heat flux forcing are also important in the early development and the decay of the events, respectively. Furthermore, neither Ashok et al. nor Kug et al. discussed the importance of subtropical forcing to these nonconventional events. This is likely because their analyses focused primarily on the SST evolutions in the tropical Pacific and the peak phase of these events.

Our study concludes that interannual SLP variability in the subtropics causes trade wind variations to initiate Type-2 SST variability in the central equatorial Pacific. The origin of the interannual SLP variability deserves a separate study and is not addressed here. Nevertheless, we want to point out that, in addition to winter hemisphere

atmospheric transient variability (such as the North Pacific Oscillation suggested by Vimont et al. 2003), a possible source of the subtropical SLP variability is the influence from the Indian–Australian monsoons, which also exhibit a strong quasi-biennial periodicity (Meehl and Arblaster 2001, 2002). We find the correlation coefficient between our subtropical high index and the Indian monsoon circulation index of Webster and Yang (1992) is 0.55 and is 0.46 between the subtropical high index and the Type-2 SST index. These relatively high correlations imply close associations among these three climate phenomena on biennial time scales. The recent modeling study of Yu et al. (2009) showed that reducing biennial variability in the Indian and Australian monsoons in a numerical experiment with the NCAR Community Climate System Model 3.0 significantly reduced the biennial SST variability produced by that model in the central equatorial Pacific. Further investigations on how the subtropics-related Type-2 SST variability studied here is involved in the establishment of so-called tropospheric biennial oscillation (TBO) are clearly warranted.

Acknowledgments. We thank two anonymous reviewers and Dr. Shang-Ping Xie for their constructive and helpful comments. This research was support by NSF Grant ATM-0925396, NASA Grant NNX06AF49H, and JPL Subcontract 1290687. The GECCO data was downloaded from http://www.ecco-group.org. Data analyses were performed at University of California, Irvine's Earth System Modeling Facility.

REFERENCES

An, S.-I., and F.-F. Jin, 2004: Nonlinearity and asymmetry of ENSO. *J. Climate,* **17,** 2399–2412.

Anderson, B. T., 2003: Tropical Pacific sea-surface temperatures and preceding sea level pressure anomalies in the subtropical North Pacific. *J. Geophys. Res.,* **108,** 4732, doi:10.1029/2003JD003805.

Ashok, K., S. Behera, S. A. Rao, H. Weng, and T. Yamagata, 2007: El Niño Modoki and its possible teleconnection. *J. Geophys. Res.,* **112,** C11007, doi:10.1029/2006JC003798.

Barnett, T. P., 1991: The interaction of multiple time scales in the tropical climate system. *J. Climate,* **4,** 269–285.

Battisti, D. S., and A. C. Hirst, 1989: Interannual variability in the tropical atmosphere–ocean system: Influence of the basic state, ocean geometry, and nonlinearity. *J. Atmos. Sci.,* **46,** 1687–1712.

Bjerknes, J., 1966: A possible response of the atmospheric Hadley circulation to equatorial anomalies of ocean temperature. *Tellus,* **18,** 820–829.

——, 1969: Atmospheric teleconnections from the equatorial Pacific. *Mon. Wea. Rev.,* **97,** 163–172.

Chang, P., L. Zhang, R. Saravanan, D. J. Vimont, J. C. H. Chiang, L. Ji, H. Seidel, and M. K. Tippett, 2007: Pacific meridional mode and El Niño–Southern Oscillation. *Geophys. Res. Lett.,* **34,** L16608, doi:10.1029/2007GL030302.

Chiang, J. C. H., and D. J. Vimont, 2004: Analogous Pacific and Atlantic meridional modes of tropical atmosphere–ocean variability. *J. Climate,* **17,** 4143–4158.

Gu, D., and S. G. H. Philander, 1995: Secular changes of annual and interannual variability in the Tropics during the past century. *J. Climate,* **8,** 864–876.

Jiang, N., J. D. Neelin, and M. Ghil, 1995: Quasi-quadrennial and quasi-biennial variability in the equatorial Pacific. *Climate Dyn.,* **12,** 101–112.

Kalnay, E., and Coauthors, 1996: The NCEP/NCAR 40-Year Reanalysis Project. *Bull. Amer. Meteor. Soc.,* **77,** 437–471.

Kao, H.-Y., and J.-Y. Yu, 2009: Contrasting eastern-Pacific and central-Pacific types of ENSO. *J. Climate,* **22,** 615–632.

Kim, S. B., T. Lee, and I. Fukumori, 2007: Mechanisms controlling the interannual variation of mixed layer temperature averaged over the Niño-3 region. *J. Climate,* **20,** 3822–3843.

Kohl, A., D. Dommenget, K. Ueyoshi, and D. Stammer, 2006: The global ECCO 1952 to 2001 ocean synthesis. ECCO Tech. Rep. 40, 44 pp. [Available online at http://www.ecco-group.org/ecco1/reports.html.]

Kug, J. S., F. F. Jin, and S. I. An, 2009: Two types of El Niño events: Cold tongue El Niño and warm pool El Niño. *J. Climate,* **22,** 1499–1515.

Larkin, N. K., and D. E. Harrison, 2005: Global seasonal temperature and precipitation anomalies during El Niño autumn and winter. *Geophys. Res. Lett.,* **32,** L16705, doi:10.1029/2005GL022860.

Lee, T., and I. Fukumori, 2003: Interannual to decadal variation of tropical–subtropical exchange in the Pacific Ocean: Boundary versus interior pycnocline transports. *J. Climate,* **16,** 4022–4042.

McCreary, J. P., and P. Lu, 1994: Interaction between the subtropical and equatorial ocean circulations: The subtropical cell. *J. Phys. Oceanogr.,* **24,** 466–497.

McPhaden, M. J., 2002: Mixed layer temperature balance on intraseasonal timescales in the equatorial Pacific Ocean. *J. Climate,* **15,** 2632–2647.

Meehl, G. A., and J. M. Arblaster, 2001: The tropospheric biennial oscillation and Indian monsoon rainfall. *Geophys. Res. Lett.,* **28,** 1731–1734.

——, and ——, 2002: The tropospheric biennial oscillation and Asian–Australian monsoon rainfall. *J. Climate,* **15,** 722–744.

Rasmusson, E. M., and T. H. Carpenter, 1982: Variations in tropical sea-surface temperature and surface wind fields associated with the Southern Oscillation/El-Niño. *Mon. Wea. Rev.,* **110,** 354–384.

——, X. Wang, and C. F. Ropelewski, 1990: The biennial component of ENSO variability. *J. Mar. Syst.,* **1,** 71–90.

Rayner, N. A., D. E. Parker, E. B. Horton, C. K. Folland, L. V. Alexander, D. P. Rowell, E. C. Kent, and A. Kaplan, 2003: Global analyses of sea surface temperature, sea ice, and night marine air temperature since the late nineteenth century. *J. Geophys. Res.,* **108,** 4407, doi:10.1029/2002JD002670.

Schopf, P. S., and M. J. Suarez, 1988: Vacillations in a coupled ocean–atmosphere model. *J. Atmos. Sci.,* **45,** 549–566.

Suarez, M. J., and P. S. Schopf, 1988: A delayed action oscillator for ENSO. *J. Atmos. Sci.,* **45,** 3283–3287.

Trenberth, K. E., and D. P. Stepaniak, 2001: Indices of El Niño evolution. *J. Climate,* **14,** 1697–1701.

Vimont, D. J., J. M. Wallace, and D. S. Battisti, 2003: The seasonal footprinting mechanism in the Pacific: Implications for ENSO. *J. Climate,* **16,** 2668–2675.

Wang, B., and Y. Wang, 1996: Temporal structure of the Southern Oscillation as revealed by a waveform and a wavelet transform. *J. Climate,* **9,** 1586–1598.

Webster, P. J., and S. Yang, 1992: Monsoon and ENSO: Selectively interactive systems. *Quart. J. Roy. Meteor. Soc.,* **118,** 877–926.

Ye, Z., and W. W. Hsieh, 2008: Changes in ENSO and associated overturning circulations from enhanced greenhouse gases by the end of the twentieth century. *J. Climate,* **21,** 5745–5763.

Yu, J.-Y., and C. R. Mechoso, 2001: A coupled atmosphere–ocean GCM study of the ENSO cycle. *J. Climate,* **14,** 2329–2350.

——, and H.-K. Kao, 2007: Decadal changes of ENSO persistence barrier in SST and ocean heat content indices 1958-2001. *J. Geophys. Res.,* **112,** D13106, doi:10.1029/2006JD007654.

——, F. Sun, and H.-Y. Kao, 2009: Contributions of Indian Ocean and monsoon biases to the excessive biennial ENSO in CCSM3. *J. Climate,* **22,** 1850–1858.

Zhang, Y., J. M. Wallace, and D. S. Battisti, 1997: ENSO-like interdecadal variability: 1900–93. *J. Climate,* **10,** 1004–1020.